Ethanol Conversion into 1,3-Butadiene by Lebedev Method over MTaSiBEA Zeolites (M= Ag, Cu, Zn)

Pavlo I. Kyriienko, Olga V. Larina, Sergiy O. Soloviev, Svitlana M. Orlyk, Christophe Calers, Stanislaw Dzwigaj

Ethanol Conversion into 1,3-Butadiene by Lebedev Method over MTaSiBEA Zeolites (M= Ag, Cu, Zn)

Pavlo I. Kyriienko,[*,†] *Olga V. Larina,*[†] *Sergiy O. Soloviev,*[†] *Svitlana M. Orlyk,*[†] *Christophe Calers,*[‡] *Stanislaw Dzwigaj*[*,‡]

[†] L.V.Pisarzhevsky Institute of Physical Chemistry of the NAS of Ukraine, 31 Prosp. Nauky, 03028 Kyiv, Ukraine.

[‡] Sorbonne Universités, UPMC Univ Paris 06, CNRS, UMR 7197, Laboratoire de Réactivité de Surface, F-75005, Paris, France.

* E-mails: pavlo_kyriienko@ukr.net (P.K.) and stanislaw.dzwigaj@upmc.fr (S.D.).

KEYWORDS: BEA zeolite, Tantalum, Copper, Silver, Zinc, Ethanol, 1,3-Butadiene

ABSTRACT:

Tantalum-containing SiBEA zeolite with isolated framework mononuclear Ta(V) doped with Ag, Cu and Zn were prepared and characterized by XRD, XPS, DR UV-VIS and FTIR (with pyridine, 2,6-di-tert-butylpyridine, pyrrole and deuterated chloroform). The conversion of ethanol as renewable raw material into 1,3-butadiene by Lebedev method over these zeolite catalysts was investigated.

The doping of TaSiBEA with Ag, Cu and Zn changes its catalytic properties in ethanol conversion into 1,3-butadiene as a result of modification of acid-base properties with formation

of additional dehydrogenation sites. Such modification allows accelerating ethanol dehydrogenation to acetaldehyde and subsequent steps of the ethanol-to-butadiene process. Ethanol conversion and butadiene selectivity over the catalysts increase in the order: TaSiBEA < ZnTaSiBEA < AgTaSiBEA < CuTaSiBEA. Higher selectivity to butadiene (73 %) was achieved over CuTaSiBEA (at 88% ethanol conversion, T = 598 K, WHSV = 0.5 h^{-1}).

INTRODUCTION

Production of chemicals from renewable raw materials, such as bio-ethanol obtained by recycling of vegetable biomass, is a major focus in sustainable chemistry and technology.[1–3] The interest of researchers is caused by the search for alternative non-fossil sources of hydrocarbons and importance of CO_2 utilization. For example, straightforward calculations based on chemical reactions show that 4 moles of CO_2 are recycled during biomass photosynthesis per 1 mole of BD. Given the global demand for BD in 2015 (12 Mt)[4], the replacement of petroleum-based process by bio-ethanol one allows utilizing of 39 Mt of CO_2 per annum (details in the Supporting Information).

1,3-Butadiene (BD), the monomer of synthetic rubbers and polymers, is one of the most important unsaturated hydrocarbons. There are two methods of BD production: Lebedev - conversion of ethanol (EtOH) over one catalyst in one reactor, and Ostromisslensky - conversion of a mixture of EtOH and acetaldehyde (AA), which is produced over a catalyst in the first reactor and then converted to BD over another catalyst in the second reactor.[5–7] These methods are perspective for practical use as alternatives to BD production from petroleum.[4,8,9] Analysis of economic and environmental aspects of realization of EtOH conversion into BD, made by Cespi et al. [4], indicates that Lebedev method is more perspective than Ostromisslensky one.

Scheme 1 shows an overall way of EtOH conversion into BD (Lebedev process)[1,4-6], including (**1**) AA formation from EtOH; (**2**) aldol condensation of AA to crotonaldehyde; (**3**) Meerwein–Ponndorf–Verley (MPV) reduction of crotonaldehyde with EtOH to crotyl alcohol and AA; and (**4**) dehydration of crotyl alcohol to 1,3-butadiene. BD selectivity of the process depends on the nature, strength and amount of acidic and basic sites on catalyst surface.[10–12]

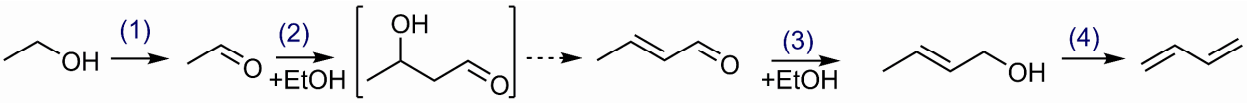

Scheme 1. Overall way of ethanol conversion into 1,3-butadiene by Lebedev method

Mixed acid-base binary oxide compositions, e.g. SiO_2 with MgO, ZrO_2 or Al_2O_3, modified with d-metal (Zn, Cu, Co, Mn, Fe, Ag) compounds, are traditional catalysts for Lebedev process.[5,13–19]

It has been found recently,[20–25] zeolite systems could be promising catalysts of the EtOH-to-BD process. Ivanova with colleagues[21] have shown that material based on ZrBEA zeolite is more active in EtOH-to-BD process than Zr-loaded SiO_2 and ordered mesoporous silica because of higher amount of LAS on the catalyst surface. It should be pointed that catalysts based on ZrBEA prepared by the post-synthesis method of zirconium planting in the zeolite matrix have similar BD selectivity in EtOH conversion by Lebedev method as ZrBEA synthesized in a fluoride medium.[24]

We have showed the conversion of EtOH and AA mixture into BD (Ostromisslensky process) proceeds with high selectivity (80 – 90 %) over tantalum-silicate zeolite (TaSiBEA) catalysts.[23] However, deficiency of active sites of EtOH dehydrogenation (step **1**) may be the cause of observed low selectivity of BD formation in Lebedev process over TaSiBEA catalyst (12–29 %).

This work shows that high butadiene selectivity is achieved in ethanol conversion by Lebedev method over TaSiBEA zeolite modified with Ag, Cu and Zn. This approach allows combining

the advantages of Lebedev (economic and environmental) and Ostromisslensky (high selectivity) methods.

EXPERIMENTAL DETAILS

Catalysts preparation. TaSiBEA, AgTaSiBEA, CuTaSiBEA and ZnTaSiBEA zeolites were prepared by two-step postsynthesis method developed earlier by Dzwigaj et al. for incorporation of vanadium atoms into BEA zeolite.[26] It consists in dealumination of a tetraethylammonium BEA (TEABEA) (Si/Al = 17) by treatment in a 13 mol · L^{-1} HNO_3 solution at 353 K for 4 h with subsequent introduction of tantalum in resulting SiBEA (with Si/Al ratio of 1300) by stirring for 3 h at 353 K in 200 ml of isopropanol solution containing 1.1×10^{-3} mol·L^{-1} $Ta(OC_2H_5)_5$ (Acros Organic, 99.99 %). The obtained suspension (pH = 6.8) was stirred in evaporator under vacuum of a water pump in air at 353 K for 1 h until isopropanol was evaporated. The resulting solids, washed three times in distilled water and dried in air at 353 K for 24 h, were finally calcined at 773 K in flowing air for 3 h. The sample is white and contain 1.0 wt % of Ta and is labeled as TaSiBEA.

Then 2 g of TaSiBEA was stirred under aerobic condition for 2 h at 298 K in 200 ml of **i**) aqueous $AgNO_3$ solution (pH = 3.7) with concentration of 0.6×10^{-3} mol·L^{-1} to obtain AgTaSiBEA zeolite with 1.0 wt % of Ag, **ii**) aqueous $Cu(NO_3)_2 \times 3H_2O$ solution (pH = 3.7) with concentration of 0.8×10^{-3} mol·L^{-1} to obtain CuTaSiBEA zeolite with 1.0 wt % of Cu, and **iii**) aqueous $Zn(NO_3)_2 \times 6H_2O$ solution (pH = 3.5) with concentration of 0.7×10^{-3} mol·L^{-1} to obtain ZnTaSiBEA zeolite with 1.0 wt % of Zn and Ta. The obtained suspensions were stirred in evaporator under vacuum of a water pump for 2 h in air at 353 K until the water was evaporated and calcined at 773 K in flowing air for 3 h. The resulting solids containing 1.0 wt % of each metal were labeled as AgTaSiBEA, CuTaSiBEA and ZnTaSiBEA.

AgSiBEA sample with 1.0 wt % of Ag, prepared according to the procedure described previously[27], was mixed with TaSiBEA sample to obtain the mechanical mixture of AgSiBEA and TaSiBEA with the ratio of Ag/Ta equivalent to that in AgTaSiBEA sample.

Catalysts characterization. The chemical analysis of the samples was performed with inductively coupled plasma atom emission spectroscopy at the CNRS Centre of Chemical Analysis (Vernaison, France).

XRD patterns of the powder samples were recorded using D8 Advance (Bruker AXS GmbH, Germany) diffractometer with monochromatized Cu-Kα radiation (nickel filter, $\lambda = 0.15418$ nm).

Diffuse reflectance (DR) UV-VIS spectra were recorded at ambient atmosphere on a Cary 5000 (Varian, USA) spectrometer equipped with a double integrator with polytetrafluoroethylene as reference.

The XP spectra were taken using an Omicron (ESCA+) X-ray photoelectron spectrometer. The base pressure in the experimental chamber was in the low 10^{-9} mbar range. The spectra were collected using a monochromatic Al Kα ($h\nu = 1486.6$ eV) X-ray source with an accelerating voltage of 14 kV and a current intensity of 20 mA. The pass energy was 20 eV for the high resolution spectra and 100 eV for the surveys. Surface charging effects were compensated by referencing the BE (binding energy) to the C 1s line of residual carbon set at 284.7 eV BE.

TEM micrographs were obtained on TEM-125 K (SELMI) microscope operating at 100 kV. For TEM measurements samples were dispersed in acetone with ultrasound and deposited on Cu grid covered with carbon. Interplanar d_{hkl} spacings calculated from the diffraction ring pattern were compared with the ASTM data.

Analysis of acid-base properties of the zeolite catalysts was performed by adsorption of pyridine, 2,6-di-tert-butylpyridine (DTBP), pyrrole and deuterated chloroform ($CDCl_3$) followed by infrared spectroscopy. FTIR spectra were recorded on a Spectrum One FTIR spectrometer

(Perkin Elmer, USA) accumulating 48 scans at a spectral resolution of 1 cm^{-1}. The samples after catalytic tests were pressed at ~ 2 ton · cm^{-2} into thin wafers of ca. 12 mg · cm^{-2}, and placed inside IR cells. Before adsorption of pyridine, DTBP and pyrrole, the IR cell was connected to a vacuum-adsorption apparatus allowing a residual pressure below 10^{-3} Pa and the samples were outgassed at 673 K for 1 h. The spectra were recorded under ambient conditions after pyridine desorption at 423 and 523 K, after DTBP desorption at 353, 423 and 523 K and after pyrrole desorption at 338 K. Before adsorption of $CDCl_3$ the catalyst-containing IR cell was heated in a constant Ar flow (~ 60 mL·min^{-1}). Once 723 K was reached, treatment lasted 1 h. Then, the samples were cooled to 323 K, and baselines were recorded. To carry the probe molecule to the IR cell Ar was passed through the $CDCl_3$-containing gas bubbler for 30 min. After that, Ar was passed through the IR cell for 30 min to avoid physical adsorbed $CDCl_3$. The spectra of adsorbed $CDCl_3$ were recorded. All measured spectra were recalculated to a "normalized" wafer weight. The height of each peak above the baseline was extracted from the experimental raw data.

Catalytic activity measurement. Catalytic activity tests were carried out in a fixed-bed flow quartz reactor with inner diameter of 4 mm at 598–673 K and atmospheric pressure. Samples with grains of 0.25–0.5 mm were loaded into the reactor (0.25 g for TaSiBEA and MTaSiBEA, 0.5 g for the mixture of AgSiBEA and TaSiBEA). Argon was used as the carrier gas (5–15 mL·min^{-1}). Before the reaction samples were heated to 673 K under flowing argon, and treatment lasted 1 h. EtOH were fed into the catalytic reactor by passing argon through temperature controlled bubbler (314 K) with 95% alcohol. Weight hourly space velocity (WHSV) was 0.5-1.5 $g_{EtOH}·g_{cat}^{-1}·h^{-1}$. The reagent and reaction products were analyzed on a gas chromatograph (KristalLyuks 4000M, MetaChrome) equipped with a TCD detector and a packed column (10 % $NiSO_4$ on coal, 3 m × 3 mm) for CO, CO_2, and a FID detector and a capillary column (HP-FFAP, 50 m × 0.32 mm) for organic compounds. Carbon balance was calculated as

total carbon amount in the analyzed products, divided by the initial total amount of carbon, and it was generally higher than 95 %.

Catalytic activity was characterized by the conversion of EtOH (**X**), selectivity to products ($\mathbf{S_i}$), BD yield ($\mathbf{Y_{BD}}$) and BD productivity ($\mathbf{P_{BD}}$):

$$X = \frac{n^0_{EtOH} - n_{EtOH}}{n^0_{EtOH}} \cdot 100\%,$$

$$S_i = \frac{n_i}{(n^0_{EtOH} - n_{EtOH})} \cdot 100\%,$$

$$Y_{BD} = \frac{X \cdot S_{BD}}{100\%},$$

$$P_{BD} = \frac{Y_{BD} \cdot WHSV \cdot 0.587}{100\%},$$

where $\mathbf{n^0_{EtOH}}$ is the initial amount of C moles of EtOH; $\mathbf{n_{EtOH}}$ and $\mathbf{n_i}$ are the amount of C moles of unreacted EtOH and product **i** in the stream of the reaction products, respectively; **0.587** is the maximum possible amount of BD (g) that can be produced from 1 g of EtOH.

Since the EtOH to BD process is characterized by carbonization and deposition of various polymerization products, a regeneration of catalyst was required after each operation cycle. The regeneration was carried out by heating the catalysts in an oxygen-containing flow (5 % O_2 in Ar, 30 ml/min) to 773 K, and treatment lasted 2 h. For each catalyst sample several cycles of catalysis were carried out, the original (initial) catalyst activity is restored after regeneration.

RESULTS AND DISCUSSION

Characterization of MTaSiBEA zeolites by XRD, DR UV-VIS and XPS. X-ray diffraction (XRD) patterns of as-prepared SiBEA, TaSiBEA and MTaSiBEA (M = Ag, Cu, Zn) (Fig. 1) are typical of BEA zeolite. It suggests that the doping of TaSiBEA with Ag, Cu and Zn does not significantly affect the zeolite crystallinity. The large increase of d_{302} spacing, calculated from

the corresponding 2θ value, from 3.920 Å (SiBEA; 2θ = 22.68°) to 3.948 Å (TaSiBEA; 2θ = 22.51°) is related to incorporation of tantalum into SiBEA. The zeolite matrix expansion occurs due to longer Ta–O bond length (1.90 Å for mononuclear Ta(V) species in BEA zeolite[28]) than Si–O (1.60–1.65 Å in zeolites).[29] In the case of MTaSiBEA d_{302} spacing is changed from 3.920 Å (SiBEA; 2θ = 22.68°) to 3.960 Å (AgTaSiBEA; 2θ = 22.38°) and to 3.931 Å (CuTaSiBEA and ZnTaSiBEA; 2θ = 22.61°), showing zeolites matrix expansion, in line with our earlier report.[27,30–32]

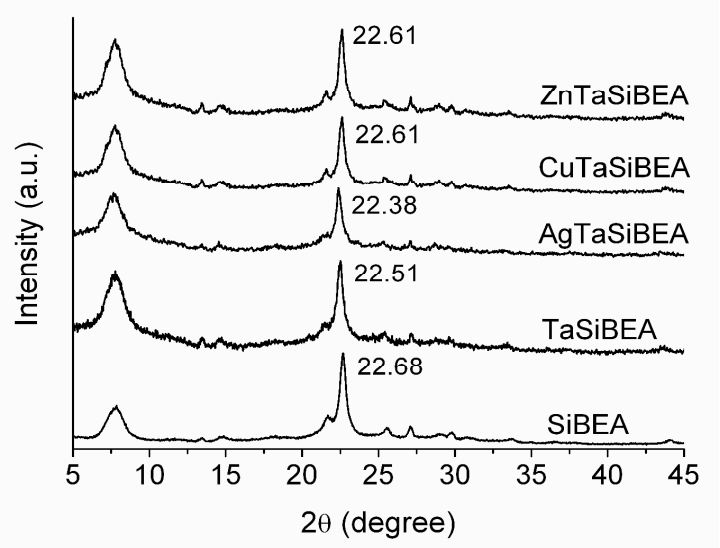

Figure 1. XRD patterns of as-prepared TaSiBEA, AgTaSiBEA, CuTaSiBEA and ZnTaSiBEA zeolites recorded at room temperature and ambient atmosphere.

DR UV-VIS spectra of SiBEA, TaSiBEA and MTaSiBEA zeolites after catalytic tests are shown in Fig. 2. The energy of oxygen-to-metal charge transfer (CT) which depends on the number oxygen atoms surrounding of the metal ion can be used to evaluate the coordination of tantalum, silver, copper and zinc in the samples.

In the spectrum of SiBEA absorption band at 208 nm are probably related to CT transitions in the BEA framework. For TaSiBEA the high-energy ligand-to-metal CT transition is centered at 216 nm, indicating the presence of mononuclear Ta(V) in the zeolite matrix.[28,33,34]

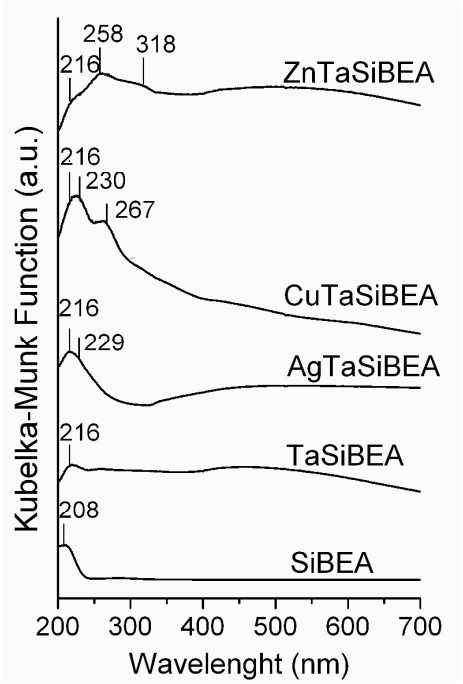

Figure 2. DR UV–VIS spectra of SiBEA, TaSiBEA, AgTaSiBEA, CuTaSiBEA and ZnTaSiBEA zeolites after catalytic tests recorded at room temperature and ambient atmosphere.

In the spectrum of AgTaSiBEA the bands at 216 and 229 nm are attributed to CT between $4d^{10}$ and $4d^{9}5s^{1}$ levels of Ag(I) species and oxidized silver clusters ($Ag_n^{\delta+}$, where $n \leq 10$), respectively.[27,35,36] Charge transfer in large Ag clusters or nanoparticles induces appearance of bands at higher wavelengths (above 350 nm), as was shown for Ag-MFI, Ag-BEA, Ag-MOR.[37] The absence of these bands suggests that these Ag species are not present in AgTaSiBEA. The band at 216 nm is more intensive on AgTaSiBEA spectrum compared to TaSiBEA, suggesting the superposition of the bands related to the presence of both isolated mononuclear Ta(V) and Ag(I) species.

In the spectrum of CuTaSiBEA the bands at the range of 216-267 nm could be attributed to CT transitions between O^{2-} and isolated mononuclear Ta^{5+} and Cu^{2+} species and oxidized copper clusters.[28,30,31,33,34] The absence of the bands in the range of 300-600 nm (Fig. 2) assigned to the

$O^{2-} \rightarrow Cu^{2+}$ CT and/or d-d transitions of octacoordinated Cu(II) indicates the absence of any bulk metal oxides on the surface of CuTaSiBEA.[38]

The appearance of absorption bands below 230 nm are generally considered as the distinguishing proof of zinc atoms incorporation into zeolite framework by isomorphous substitution, in agreement with earlier report.[39] Pure ZnO gives broad adsorption band at about 360 nm, assigned to the $O^{2-} \rightarrow Zn^{2+}$ CT transition between oxygen and zinc in oxide.[40] The bands in the range of 216-360 nm on the spectrum of ZnTaSiBEA (Fig. 2) are attributed to mononuclear Ta(V) species (216 nm)[28,33,34], isolated mononuclear framework Zn(II) (258 nm)[39] and polynuclear zinc oxide present in the extra-framework position (318 nm).[40]

XPS was used to determine the valence state of tantalum, silver, copper, and zinc in MTaSiBEA catalysts before and after catalytic tests. The results of curve-fitting of the obtained XP spectra are presented in Table 1 (the XP spectra are shown on Figs S1-S3).

The XP spectra of MTaSiBEA (Figs S1a, S2a and S3a) in the Ta $4f_{5/2}$ and $4f_{7/2}$ range show two intensive signals at about 29.1-29.2 and 24.8-25.2 eV, respectively, characteristic of Ta(V) species well dispersed in zeolite matrix.[41] Fig. S1b shows the Ag $3d_{3/2}$ (374.6 eV) and $3d_{5/2}$ (368.65 eV) bands, indicating that Ag^{+} and $Ag_n^{\delta+}$ are main silver species in AgTaSiBEA.[42,43] In the case of CuTaSiBEA (Fig. S2b), the bands at 953.3 eV in the $2p_{1/2}$ range and 933.3 eV in the $2p_{3/2}$ range are characteristic of well dispersed Cu(II) strongly interacting with BEA zeolite matrix.[31,44]

Two intensive bands at 1045.5 eV and 1022.5 eV were observed on the XP spectrum of ZnTaSiBEA in the Zn $2p_{1/2}$ and Zn $2p_{3/2}$ ranges (Fig. S3b), which may be attributed to dispersed Zn(II) species present in the zeolite structure.[45] The BE of the peak in the Zn $2p_{3/2}$ range of 1022.5 eV strongly suggest that zinc is present in ZnTaSiBEA in the framework position, in agreement with earlier report on framework zinc substituted zeolites.[46]

BEs of Ta $4f_{5/2}$ and $4f_{7/2}$, Ag $3d_{3/2}$ and $3d_{5/2}$, Cu $2p_{1/2}$ and $2p_{3/2}$, Zn $2p_{1/2}$ and Zn $2p_{3/2}$ for spent-MTaSiBEA differ slightly (max 0.3 eV) from fresh samples (Table 1). Insignificant changes of valence state of tantalum, silver, copper and zinc in the catalysts suggest the stability of Ta(IV), Ag(I), Cu(II) and Zn(II) species in MTaSiBEA framework after EtOH-to-BD catalytic runs.

Table 1. XPS results for MTaSiBEA zeolites

Catalysts	Binding energy (eV)			
AgTaSiBEA	*Ag $3d_{3/2}$*	*Ag $3d_{5/2}$*	*Ta $4f_{5/2}$*	*Ta $4f_{7/2}$*
fresh	374.6	368.6	29.2	25.2
spent	374.5	368.5	29.0	24.9
CuTaSiBEA	*Cu $2p_{1/2}$*	*Cu $2p_{3/2}$*	*Ta $4f_{5/2}$*	*Ta $4f_{7/2}$*
fresh	953.3	933.5	29.1	24.8
spent	953.1	933.3	28.9	24.7
ZnTaSiBEA	*Zn $2p_{1/2}$*	*Zn $2p_{3/2}$*	*Ta $4f_{5/2}$*	*Ta $4f_{7/2}$*
fresh	1045.5	1022.5	29.2	25.0
spent	1045.5	1022.4	29.0	24.9

Under reaction conditions (603 K, presence of H_2, EtOH, AA) reduction of extra-framework oxidized species might have been expected.[27,47] However, XPS and DR-UV-VIS results for spent-samples demonstrate the presence of highly dispersed mononuclear Ta(V), Ag(I), Cu(II) and Zn(II). Apparently, these species are easily oxidized in air at ambient conditions during the replacement into XPS/DR-UV-VIS chambers and/or species strongly bonded or incorporated in the framework are not reduced in the reaction conditions. Moreover, reduction of zinc oxide occurs at temperatures above 823 K.[48]

On the TEM images of MTaSiBEA calcined at 773 K (Supporting Information, Fig. S4) no bulk metal oxides and/or metal particles of tantalum, silver, copper and zinc are seen. No clear ring diffraction patterns of tantalum, silver, copper and zinc are visible which may indicate high dispersion of tantalum, silver, copper and zinc in the zeolites. The interplanar d_{hkl} spacings for the most contrast electron diffraction rings are equal to 3.948 Å for TaSiBEA, 3.960 Å for AgTaSiBEA and 3.931 Å for CuTaSiBEA and ZnTaSiBEA can be attributed to the (302) plane BEA zeolite that consist with the XRD results.

Thus, using the SiBEA zeolite as carrier allows stabilization of the tantalum, silver, copper and zinc as highly dispersed mononuclear Ta(V), Ag(I), Cu(II), and Zn(II) species.

FTIR characterization of acid-base sites by pyridine, DTBP, pyrrole and $CDCl_3$ adsorption. FTIR spectra of pyridine adsorbed on TaSiBEA and MTaSiBEA are presented in Fig. 3. The bands at 1611-1613, 1599-1600 and 1446-1454 cm^{-1} correspond to pyridine interacting with Lewis acidic sites (LAS), formed by incorporated metal ions, in line with earlier data for tantalum,[28,34,49] silver[27] and copper[30] in SiBEA, and zinc in MFI.[40,50] The intensity of these bands for SiBEA[27] is much lower. Thus, additional LAS are formed upon incorporation of Ta, Ag, Cu and Zn ions in the zeolite framework.

In Cu- and Zn-containing zeolites spectra bands of adsorbed pyridine are more intensive than for Ag-containing (at 523 and 623 K), which may indicate formation of higher amount of strong LAS after copper and zinc incorporation.

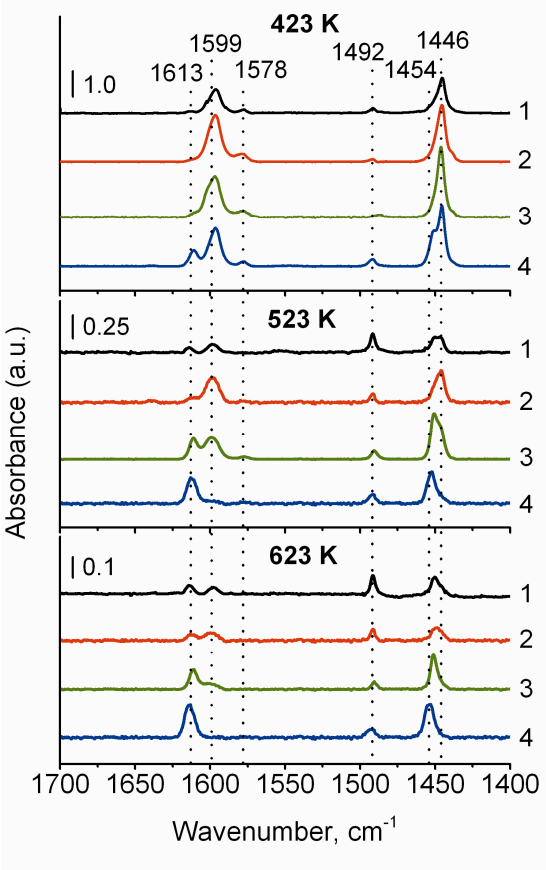

Figure 3. FTIR spectra of adsorbed pyridine on as-prepared TaSiBEA (1), AgTaSiBEA (2), CuTaSiBEA (3) and ZnTaSiBEA (4) catalysts after desorption at different temperatures.

Bands of pyridinium ions formed on Brönsted acidic sites (BAS) were not observed (1638 and 1545 cm^{-1}). Therefore, DTBP as stronger base than pyridine has been used to establish presence of weak BAS (Fig. 4). The bands at 1614 and 1530 cm^{-1} are assigned to protonated DTBP adsorbed on BAS.[34,51,52] The intensity of these bands is slightly higher for ZnTaSiBEA than for TaSiBEA indicating higher amount of BAS.

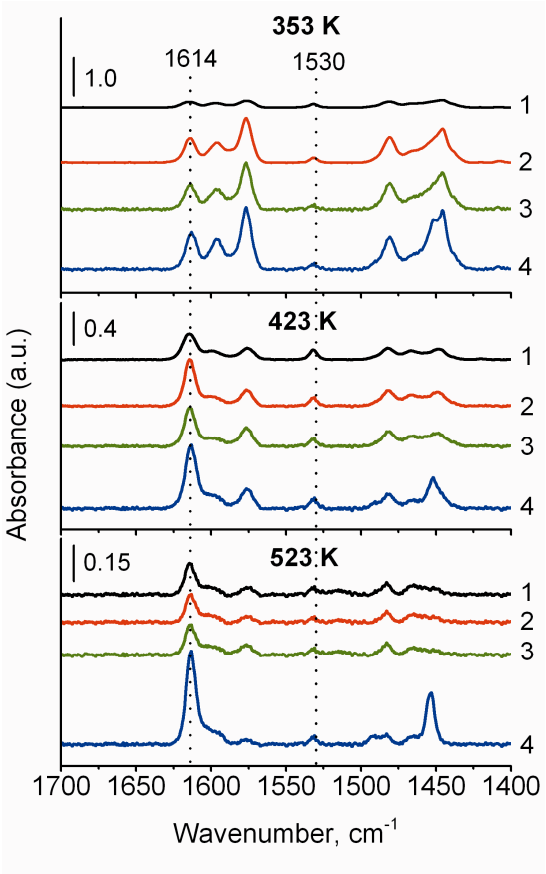

Figure 4. FTIR spectra of adsorbed DTBP on as-prepared TaSiBEA (1), AgTaSiBEA (2), CuTaSiBEA (3) and ZnTaSiBEA (4) catalysts after desorption at different temperatures.

Pyrrole and $CDCl_3$ were used as probe molecules for identification of basic sites on the surface of TaSiBEA, AgTaSiBEA, CuTaSiBEA and ZnTaSiBEA zeolites (Fig. 5). The bands at 1534, 1470, 1420 and 1379 cm^{-1} are attributed to pyrrole ring-stretching vibrations, in line with earlier reports.[53,54] The band at 3545 cm^{-1} corresponding to strongly perturbed OH vibrations of pyrrole, as well as bands at 3480 cm^{-1} combined with 1490 cm^{-1} indicates the presence of pyrrole species adsorbed on acidic sites.[53,54] The intensity of the band at 3480 cm^{-1} is high for CuTaSiBEA and ZnTaSiBEA. It is likely that copper- and zinc-containing acidic sites are stronger, in line with the FTIR data with pyridine adsorption (Fig. 3). The shoulder at 3390 cm^{-1} in the spectra of

TaSiBEA and MTaSiBEA zeolites indicates the presence of weak basic sites, in line with previous report.[53]

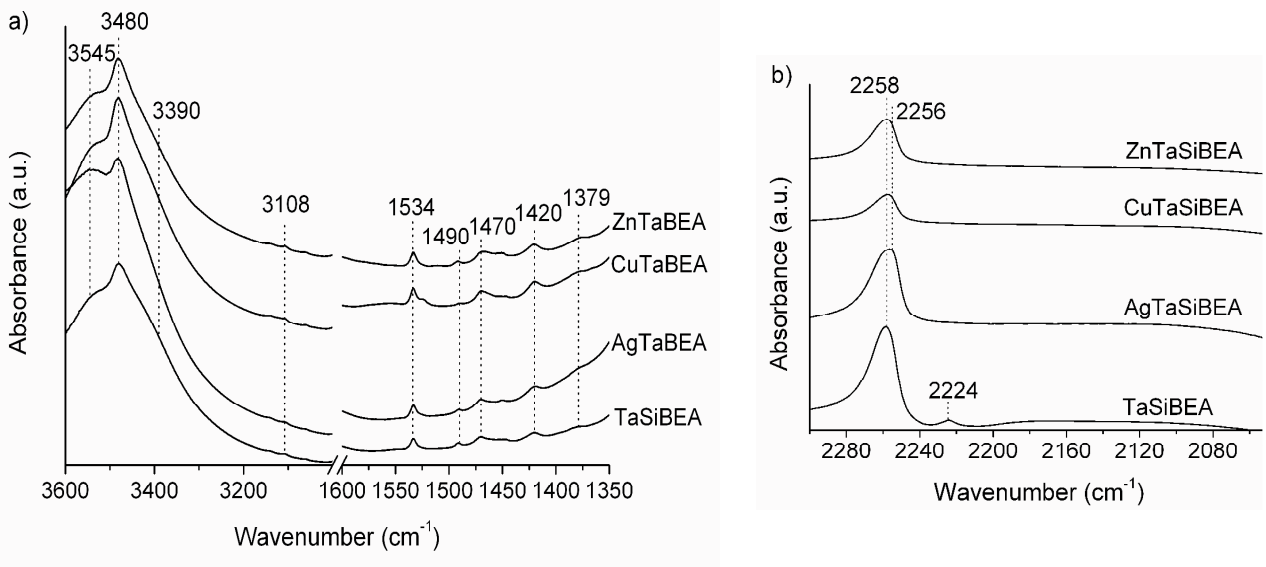

Figure 5. FTIR spectra of adsorbed pyrrole after desorption at 338 K (a) and adsorbed $CDCl_3$ after desorption at 323 K (b) on as-prepared TaSiBEA and MTaSiBEA catalysts.

FTIR spectra of $CDCl_3$ adsorbed on TaSiBEA and MTaSiBEA are presented in Fig. 5-b. The bands at 2558 and 2224 cm^{-1} in the spectra of TaSiBEA are attributed to weak and medium basic sites.[55] In the spectra of the MTaSiBEA samples only one band at 2256 cm^{-1} is present. It suggests that incorporation of Ag, Cu or Zn into TaSiBEA leads to elimination of medium basic sites and simultaneous decreasing of the number of weak basic sites. The similar phenomenon was earlier observed for CuO/SiO_2-MgO system.[55] Intensity of the band at 2258–2256 cm^{-1} depends on the kind of the metal introduced in the TaSiBEA zeolite. This band is less intense on the spectra of CuTaSiBEA and ZnTaSiBEA indicating the lower number of weak basic sites for CuTaSiBEA and ZnTaSiBEA. These data falls into line the results of FTIR spectroscopy of adsorbed pyridine and pyrrole.

Thus, the TaSiBEA and MTaSiBEA zeolites possess weak Brønsted acidic, Lewis acidic and basic sites, formed by incorporation of Ta, Ag, Cu and Zn into framework of BEA zeolite.[23]

Catalytic properties of MTaSiBEA zeolites. The main products of ethanol conversion on TaSiBEA and MTaSiBEA are BD, AA, ethylene and diethyl ether **(**DEE**) (**Table 2**)**. The formation of propylene, ethylene, ethyl acetate and other products are also observed (Table S1 in Supplementary materials). EtOH conversion over TaSiBEA does not exceed 13.3 %, and BD selectivity – 16.4 %.[23] The introduction of Ag, Cu and Zn in TaSiBEA zeolite entails substantial increase in EtOH conversion and selectivity to BD. The highest values are observed over CuTaSiBEA with EtOH conversion of 87.9 and BD selectivity of 72.6 %.

The selectivity of EtOH conversion into BD in the presence of AgTaSiBEA (Table 2) is relatively high (62.6 %). It is comparable to the value observed in the presence of Ag/ZrBEA catalysts prepared by direct and postsynthetic methods.[21,24] However, significant amount of unreacted AA remains among the reaction products, probably, because of insufficient number of acidic and basic sites with strength required for accelerate AA conversion through aldol condensation (step **2** in Scheme 1).

Table 2. Catalytic performance of TaSiBEA and MTaSiBEA zeolites in EtOH conversion[a]

Catalysts	EtOH conversion (%)	Product selectivity (C mol%)						BD yield (C mol%)
		BD	AA	croton aldehyde	ethylene	diethyl ether	other	
TaSiBEA[b]	13.3	16.4	33.0	0.1	28.3	20.8	1.4	2.2
AgTaSiBEA	82.9	62.6	23.9	0.4	7.6	0.9	4.6	51.9
CuTaSiBEA	87.9	72.6	15.0	0.2	2.7	1.0	8.5	63.8
ZnTaSiBEA	51.7	42.8	22.7	0.2	17.1	13.0	4.2	22.1
AgSiBEA+ TaSiBEA	58.3	46.0	16.2	0.1	11.9	22.1	3.7	26.8

[a] T = 598 K, WHSV = 0.5 $g_{EtOH} \cdot g_{cat}^{-1} \cdot h^{-1}$, time-on-stream = 3.5 h, [b] the data of report[23]

It should be mentioned that in the presence of AgSiBEA catalyst (obtained by the method described in earlier report[27]) EtOH conversion proceeds with predominantly formation of AA (97 % selectivity). Over mechanical mixture of AgSiBEA + TaSiBEA 46 % selectivity to BD was achieved. The much higher value of selectivity to BD in the presence of AgTaSiBEA catalyst than for mixture of AgSiBEA + TaSiBEA may be caused by proximity localization of the active sites of EtOH dehydrogenation (step **1**) and the subsequent steps (**2–4**).

In the presence of ZnTaSiBEA 51.7 % EtOH conversion occurs with 42.8 % BD selectivity (Table 2). The significant amount of ethylene and DEE was observed in the reaction products (total selectivity of 30 %). This phenomenon may be caused by higher number of BAS and LAS (Figs. 3 and 4), accelerating side reaction of EtOH dehydration.

Let us consider the origin of different effect of the dopants (Ag, Cu, Zn) on the activity and selectivity of TaSiBEA. The main role of Ag, Cu and Zn in the MTaSiBEA catalysts consists in the formation of sites of EtOH dehydrogenation and modification of acid-base characteristics of the zeolites. The mechanism of alcohol dehydrogenation over silica- and alumina-supported silver catalysts includes: 1) the activation of ethanol with formation of hydrogen-bonded surface complex on silica/alumina surface, 2) C—H bond cleavage on Ag sites and proton abstraction on silica/alumina acid-base sites (rate-determining step), and 3) desorption of H_2 and acetaldehyde, with regeneration of the active sites.[56,57] Acid-base properties of the support and nature of silver species affect the dehydrogenation process.[56,57]

As was previously shown over Ag/SiO_2 and Cu/SiO_2 EtOH is mainly converted to AA,[22] and over ZnO/SiO_2 – to ethylene with selectivity of 35 %.[18] The rate of ethanol dehydrogenation in the presence of Cu species is higher than on ZnO,[58] because dehydrogenation pathways over metallic copper and zinc oxide are different. Moreover, probability of ethanol dehydration to ethylene over ZnO is higher than over Cu species. [59] Apparently, appropriate ratio of acid-base

and redox characteristics of the catalyst is achieved by the doping of TaSiBEA with copper, and, thereby, higher yield of BD is achieved over CuTaSiBEA.

We have previously shown that high BD selectivity is maintained after repeated operation cycles on TaSiBEA.[23] EtOH conversion, BD yield and selectivity to products as a function of time-on-stream for MTaSiBEA catalysts are presented in Fig. 6. The values of EtOH conversion and BD yield noticeably reduce with time in the presence of MTaSiBEA catalysts. Higher stability in time of the EtOH conversion, selectivity and yield of BD are observed in the case of CuTaSiBEA catalyst among the studied samples (Fig. 6). It seems that the active sites formed upon the doping of TaSiBEA with copper are more stable in the process of EtOH conversion into BD. The similar results were observed in the EtOH-to-AA process over the Ag/SiO_2 and Cu/SiO_2 catalysts.[22] Stable performance of the copper-containing catalyst in this process was also demonstrated in the earlier report.[60]

Tables 3 and Fig. 7 summarize the effect of WHSV on EtOH conversion over CuTaSiBEA. Increasing of WHSV results in substantial decrease in EtOH conversion, selectivity to BD, and, as a result, BD productivity in the process. Moreover, the amount of unreacted AA as well as EtOH dehydration products (ethylene and DEE) increases significantly (side products are shown in Table S2). Similar dependence of selectivity to products in EtOH conversion on the contact time was observed for others catalytic systems.[13,61,62]

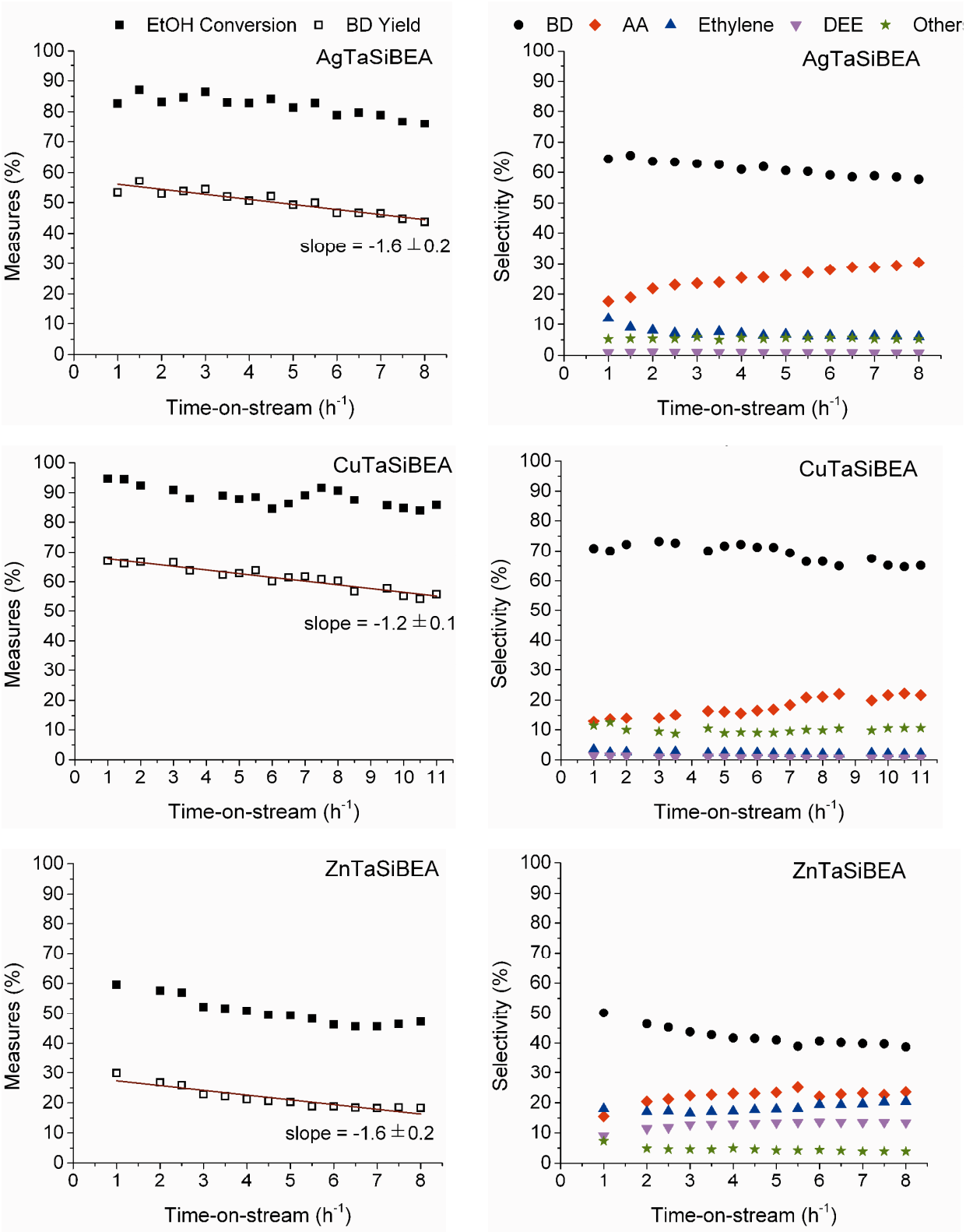

Figure 6. EtOH conversion, BD yield and selectivity to products over MTaSiBEA catalysts as function of time-on-stream (T = 598 K, WHSV = 0.5 $g_{EtOH} \cdot g_{cat}^{-1} \cdot h^{-1}$).

Table 3. Effect of WHSV on EtOH conversion over CuTaSiBEA catalyst[a]

WHSV ($g_{EtOH} \cdot g_{cat}^{-1} \cdot h^{-1}$)	EtOH conversion (%)	Product selectivity (C mol%)						BD yield (C mol %)	BD productivity ($g_{BD}\ g_{cat}^{-1}\ h^{-1}$)
		BD	AA	croton aldehyde	ethylene	diethyl ether	other		
0.5	87.9	72.6	15.0	0.2	2.7	1.0	8.5	63.8	0.19
1	52.1	52.5	23.4	0.3	6.4	9.8	7.6	27.4	0.16
1.5	30.1	44.8	28.8	0.1	12	8.4	5.9	13.5	0.12

[a] T = 598 K, time-on-stream = 3.5 h.

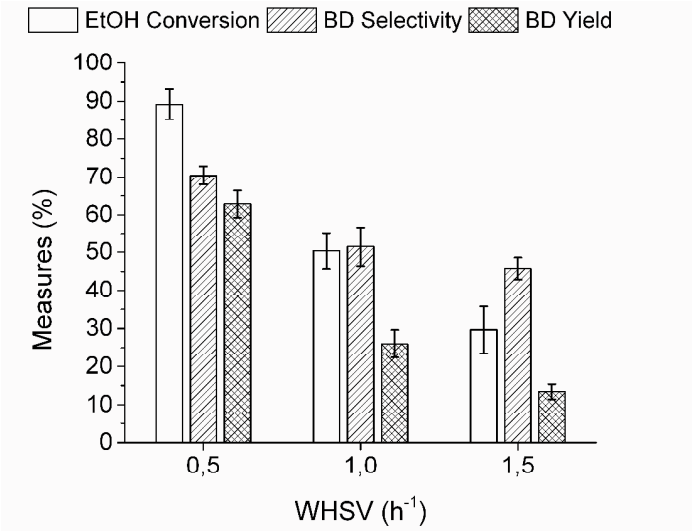

Figure 7. EtOH conversion, BD selectivity and yield over CuTaSiBEA catalyst as function of WHSV (T = 598 K). The bars represent average measures for range of 1–9 h time-on-stream.

Raise of the reaction temperature from 598 to 673 K significantly increases EtOH conversion from 30 to 65 % (Fig. 8), but selectivity to desired product (BD) is markedly reduced from 45 to 27 %. Thus, the high selectivity and yield of BD over MTaSiBEA are achieved only under definite range of parameters for process proceeding.

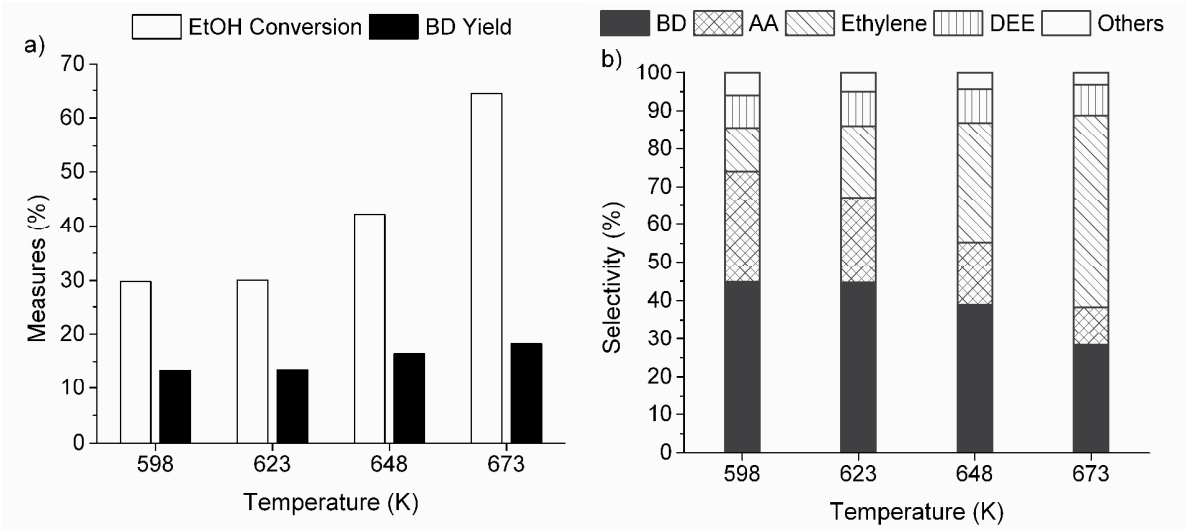

Figure 8. EtOH conversion, BD yield (a) and product selectivities (b) over CuTaSiBEA as function of temperature (WHSV=1.5 $g_{EtOH} \cdot gcat^{-1} \cdot h^{-1}$).

CONCLUSIONS

The doping of tantalum-siliceous zeolite (TaSiBEA) with Ag, Cu and Zn changes its catalytic properties in ethanol conversion into 1,3-butadiene by Lebedev method as a result of modification of acid-base properties with formation of additional dehydrogenation sites.

Such modification allows accelerating ethanol dehydrogenation to acetaldehyde and subsequent steps of the ethanol-to-butadiene process.

Ethanol conversion and butadiene selectivity over MTaSiBEA increase in the order: TaSiBEA < ZnTaSiBEA < AgTaSiBEA < CuTaSiBEA.

Higher selectivity to BD (73 %) was achieved over CuTaSiBEA (at 88% ethanol conversion, T = 598 K, WHSV = 0.5 h^{-1}), suggesting that this zeolite material could be a promising catalyst for Lebedev process.

ASSOCIATED CONTENT

Supporting Information. The details of the calculations of the amount of recycled CO_2 in 1,3-butadiene production from biomass, XP spectra, TEM images and diffraction patterns, additional catalytic results. This material is available free of charge via the Internet at http://pubs.acs.org.

AUTHOR INFORMATION

Corresponding Authors

* E-mails: pavlo_kyriienko@ukr.net (P.K.) and stanislaw.dzwigaj@upmc.fr (S.D.).

Author Contributions

The manuscript was written through contributions of all authors. All authors have given approval to the final version of the manuscript.

Acknowledgements

The authors acknowledge IMPC (Institut des Materiaux de Paris Centre, FR2482) and the C'Nano projects of the Region Ile-de-France, for Omicron XPS apparatus funding.

REFERENCES

(1) Angelici, C.; Weckhuysen, B. M.; Bruijnincx, P. C. A. Chemocatalytic conversion of ethanol into butadiene and other bulk chemicals. *ChemSusChem* **2013**, *6* (9), 1595–1614.

(2) Posada, J. A.; Patel, A. D.; Roes, A.; Blok, K.; Faaij, A. P. C.; Patel, M. K. Potential of bioethanol as a chemical building block for biorefineries: preliminary sustainability assessment of 12 bioethanol-based products. *Bioresour. Technol.* **2013**, *135*, 490–499.

(3) Sun, J.; Wang, Y. Recent Advances in Catalytic Conversion of Ethanol to Chemicals. *ACS*

Catal. **2014**, *4* (4), 1078–1090.

(4) Cespi, D.; Passarini, F.; Vassura, I.; Cavani, F. Butadiene from biomass, a life cycle perspective to address sustainability in the chemical industry. *Green Chem.* **2016**, *18*, 1625–1638.

(5) Makshina, E. V.; Dusselier, M.; Janssens, W.; Degrève, J.; Jacobs, P. A.; Sels, B. F. Review of old chemistry and new catalytic advances in the on-purpose synthesis of butadiene. *Chem. Soc. Rev.* **2014**, *43* (22), 7917–7953.

(6) Jones, M. D. Catalytic transformation of ethanol into 1,3-butadiene. *Chem. Cent. J.* **2014**, *8*, 53–58.

(7) Gallo, J. M. R.; Bueno, J. M. C.; Schuchardt, U. Catalytic Transformations of Ethanol for Biorefineries. *J. Braz. Chem. Soc.* **2014**, *25* (12), 2229–2243.

(8) Axens, IFPEN and Michelin Join Forces to Create a Synthetic Rubber Production Channel Using Biomass.

(9) Patel, A. D.; Meesters, K.; den Uil, H.; de Jong, E.; Blok, K.; Patel, M. K. Sustainability assessment of novel chemical processes at early stage: application to biobased processes. *Energy Environ. Sci.* **2012**, *5* (9), 8430–8444.

(10) Angelici, C.; Velthoen, M. E. Z.; Weckhuysen, B. M.; Bruijnincx, P. C. A. Influence of acid–base properties on the Lebedev ethanol-to-butadiene process catalyzed by SiO2–MgO materials. *Catal. Sci. Technol.* **2015**, *5* (5), 2869–2879.

(11) Ordomsky, V. V.; Sushkevich, V. L.; Ivanova, I. I. Study of acetaldehyde condensation chemistry over magnesia and zirconia supported on silica. *J. Mol. Catal. A Chem.* **2010**, *333* (1–2), 85–93.

(12) Kvisle, S.; Aguero, A.; Sneeden, R. P. A. Transformation of ethanol into 1,3-butadiene over magnesium oxide/silica catalysts. *Appl. Catal.* **1988**, *43* (1), 117–131.

(13) Makshina, E. V.; Janssens, W.; Sels, B. F.; Jacobs, P. a. Catalytic study of the conversion of ethanol into 1,3-butadiene. *Catal. Today* **2012**, *198* (1), 338–344.

(14) Ezinkwo, G. O.; Tretjakov, V. F.; Talyshinky, R. M.; Ilolov, A. M.; Mutombo, T. A. Creation of a continuous process for bio-ethanol to butadiene conversion via the use of a process initiator. *Catal. Commun.* **2014**, *43*, 207–212.

(15) Lewandowski, M.; Babu, G. S.; Vezzoli, M.; Jones, M. D.; Owen, R. E.; Mattia, D.; Plucinski, P.; Mikolajska, E.; Ochenduszko, A.; Apperley, D. C. Investigations into the conversion of ethanol to 1,3-butadiene using MgO:SiO2 supported catalysts. *Catal. Commun.* **2014**, *49*, 25–28.

(16) Sekiguchi, Y.; Akiyama, S.; Urakawa, W.; Koyama, T.; Miyaji, A.; Motokura, K.; Baba, T. One-step catalytic conversion of ethanol into 1,3-butadiene using zinc-containing talc. *Catal. Commun.* **2015**, *68*, 20–24.

(17) Angelici, C.; Velthoen, M. E. Z.; Weckhuysen, B. M.; Bruijnincx, P. C. A. Effect of preparation method and CuO promotion in the conversion of ethanol into 1,3-butadiene over SiO2-MgO catalysts. *ChemSusChem* **2014**, 2505–2515.

(18) Larina, O. V.; Kyriienko, P. I.; Soloviev, S. O. Ethanol Conversion to 1,3-Butadiene on ZnO/MgO–SiO2 Catalysts: Effect of ZnO Content and MgO:SiO2 Ratio. *Catal. Letters* **2015**, *145* (5), 1162–1168.

(19) Janssens, W.; Makshina, E. V.; Vanelderen, P.; De Clippel, F.; Houthoofd, K.; Kerkhofs, S.; Martens, J. A.; Jacobs, P. a.; Sels, B. F. Ternary Ag/MgO-SiO2 Catalysts for the Conversion of Ethanol into Butadiene. *ChemSusChem* **2015**, *8* (6), 994–1008.

(20) Sushkevich, V. L.; Palagin, D.; Ivanova, I. I. With Open Arms: Open Sites of ZrBEA Zeolite Facilitate Selective Synthesis of Butadiene from Ethanol. *ACS Catal.* **2015**, *5* (8), 4833–4836.

(21) Sushkevich, V. L.; Ivanova, I. I.; Taarning, E. Ethanol conversion into butadiene over Zr-containing molecular sieves doped with silver. *Green Chem.* **2015**, *17* (4), 2552–2559.

(22) Klein, A.; Keisers, K.; Palkovits, R. Formation of 1,3-butadiene from ethanol in a two-step process using modified zeolite-ß catalysts. *Appl. Catal. A Gen.* **2016**, *514*, 192–202.

(23) Kyriienko, P. I.; Larina, O. V.; Soloviev, S. O.; Orlyk, S. N.; Dzwigaj, S. High selectivity of TaSiBEA zeolite catalysts in 1,3-butadiene production from ethanol and acetaldehyde mixture. *Catal. Commun.* **2016**, *77*, 123–126.

(24) Sushkevich, V. L.; Ivanova, I. I. Ag-Promoted ZrBEA Zeolites Obtained by Post-Synthetic Modification for Conversion of Ethanol to Butadiene. *ChemSusChem* **2016**, *9* (16), 2216–2225.

(25) Kyriienko, P. I.; Larina, O. V.; Popovych, N. O.; Soloviev, S. O.; Millot, Y.; Dzwigaj, S. Effect of the niobium state on the properties of NbSiBEA as bifunctional catalysts for gas- and liquid-phase tandem processes. *J. Mol. Catal. A Chem.* **2016**, *424*, 27–36.

(26) Dzwigaj, S.; Peltre, M. J.; Massiani, P.; Davidson, A.; Che, M.; Sen, T.; Sivasanker, S. Incorporation of vanadium species in a dealuminated β zeolite. *Chem. Commun.* **1998**, No. 1, 87–88.

(27) Dzwigaj, S.; Millot, Y.; Krafft, J.-M.; Popovych, N. O.; Kyriienko, P. Incorporation of Silver Atoms into the Vacant T-Atom Sites of the Framework of SiBEA Zeolite as Mononuclear Ag(I) Evidenced by XRD, FTIR, NMR, DR UV–vis, XPS, and TPR. *J. Phys. Chem. C* **2013**, *117* (24), 12552–12559.

(28) Corma, A.; Llabrés I Xamena, F. X.; Prestipino, C.; Renz, M.; Valencia, S. Water resistant, catalytically active Nb and Ta isolated Lewis acid sites, homogeneously distributed by direct synthesis in a Beta zeolite. *J. Phys. Chem. C* **2009**, *113* (26), 11306–11315.

(29) Blasco, T.; Camblor, M. A.; Corma, A.; Esteve, P.; Guil, J. M.; Martı, A.; Valencia, S.; Martinez, A.; Perdigon-Melon, J. A. Direct synthesis and characterization of hydrophobic aluminum-free Ti-beta zeolite. *J. Phys. Chem. B* **1998**, *102* (1), 75–88.

(30) Dzwigaj, S.; Janas, J.; Gurgul, J.; Socha, R. P.; Shishido, T.; Che, M. Do Cu(II) ions need Al atoms in their environment to make CuSiBEA active in the SCR of NO by ethanol or propane? A spectroscopy and catalysis study. *Appl. Catal. B Environ.* **2009**, *85* (3–4), 131–138.

(31) Janas, J.; Gurgul, J.; Socha, R. P.; Dzwigaj, S. Effect of Cu content on the catalytic activity of CuSiBEA zeolite in the SCR of NO by ethanol: Nature of the copper species. *Appl. Catal. B Environ.* **2009**, *91* (1–2), 217–224.

(32) Omegna, A.; Vasic, M.; Bokhoven, J. A. Van; Pirngruber, G.; Prins, R. Dealumination and realumination of microcrystalline zeolite beta: an XRD, FTIR and quantitative multinuclear (MQ) MAS NMR study. *Phys. Chem. Chem. Phys.* **2004**, 447–452.

(33) Climent, M. J.; Corma, A.; Iborra, S. Mono- and multisite solid catalysts in cascade reactions for chemical process intensification. *ChemSusChem* **2009**, *2* (6), 500–506.

(34) Mueller, P.; Burt, S. P.; Love, A. M.; McDermott, W. P.; Wolf, P.; Hermans, I. Mechanistic Study on the Lewis-acid Catalyzed Synthesis of 1,3-Butadiene over Ta-BEA Using Modulated Operando DRIFTS-MS. *ACS Catal.* **2016**, *6*, 6823–6832.

(35) Shibata, J.; Shimizu, K. I.; Takada, Y.; Shichi, A.; Yoshida, H.; Satokawa, S.; Satsuma, A.; Hattori, T. Structure of active Ag clusters in Ag zeolites for SCR of NO by propane in the presence of hydrogen. *J. Catal.* **2004**, *227* (2), 367–374.

(36) Texter, J.; Gonsiorowski, T.; Kellerman, R. 5s←4d transition of trigonal Ag+ in zeolite. *Phys. Rev. B* **1981**, *23* (9), 4407–4418.

(37) Satsuma, A.; Shibata, J.; Wada, A.; Shinozaki, Y.; Hattori, T. In-situ UV-Visible

Spectroscopic Study for Dynamic Analysis of Silver Catalyst. *Sci. Technol. Catal.* **2003**, *145*, 235–238.

(38) Shimizu, K. I.; Maruyama, R.; Hatamachi, T.; Kodama, T. O2-bridged multicopper(II) complex in zeolite for catalytic direct photo-oxidation of benzene to diphenols. *J. Phys. Chem. C* **2007**, *111* (17), 6440–6446.

(39) Bordiga, S.; Lamberti, C.; Ricchiardi, G.; Regli, L.; Bonino, F.; Damin, A.; Lillerud, K.-P.; Bjorgen, M.; Zecchina, A. Electronic and vibrational properties of a MOF-5 metal-organic framework: ZnO quantum dot behaviour. *Chem. Commun.* **2004**, *5* (20), 2300–2301.

(40) Wang, L.; Sang, S.; Meng, S.; Zhang, Y.; Qi, Y.; Liu, Z. Direct synthesis of Zn-ZSM-5 with novel morphology. *Mater. Lett.* **2007**, *61* (8–9), 1675–1678.

(41) Reddy, R. G. .; Balasubramanian, S.; Chennakesavulu, K. Zeolite encapsulated active metal composites and their photocatalytic studies for rhodamine-B, reactive red-198 and chloro-phenols. *RSC Adv.* **2015**, *5*, 81013–81023.

(42) Hutson, N. D.; Reisner, B. A.; Yang, R. T.; Toby, B. H. Silver Ion-Exchanged Zeolites Y, X, and Low-Silica X: Observations of Thermally Induced Cation/Cluster Migration and the Resulting Effects on the Equilibrium Adsorption of Nitrogen. *Chem. Mater.* **2000**, *12* (10), 3020–3031.

(43) Ju, W.-S.; Matsuoka, M.; Iino, K.; Yamashita, H.; Anpo, M. The Local Structures of Silver(I) Ion Catalysts Anchored within Zeolite Cavities and Their Photocatalytic Reactivities for the Elimination of N2O into N2 and O2. *J. Phys. Chem. B* **2004**, *108* (7), 2128–2133.

(44) Dzwigaj, S.; Janas, J.; Mizera, J.; Gurgul, J.; Socha, R. P.; Che, M. Incorporation of copper in SiBEA zeolite as isolated lattice mononuclear Cu(II) species and its role in

selective catalytic reduction of NO by ethanol. *Catal. Letters* **2008**, *126* (1–2), 36–42.

(45) Gong, T.; Qin, L.; Lu, J.; Feng, H. ZnO modified ZSM-5 and Y zeolites fabricated by atomic layer deposition for propane conversion. *Phys. Chem. Chem. Phys.* **2015**, *18*, 601–614.

(46) Hunsicker, R. A.; Klier, K.; Gaffney, T. S.; Kirner, J. G. Framework Zinc-Substituted Zeolites: Synthesis, and Core-Level and Valence-Band XPS. *Chem. Mater.* **2002**, *13* (5), 4807–4811.

(47) Baran, R.; Grzybek, T.; Onfroy, T.; Dzwigaj, S. High activity of mononuclear copper present in the framework of CuSiBEA zeolites in the selective catalytic reduction of NO with NH3. *Microporous Mesoporous Mater.* **2016**, *226*, 104–109.

(48) Sasaoka, E.; Hirano, S.; Kasaoka, S.; Sakata, Y. Stability of Zinc-Oxide High-Temperature Desulfurization Sorbents for Reduction. *Energy & Fuels* **1994**, *8* (3), 763–769.

(49) Tielens, F.; Shishido, T.; Dzwigaj, S. What do tantalum framework sites look like in zeolites? A combined theoretical and experimental investigation. *J. Phys. Chem. C* **2010**, *114* (21), 9923–9930.

(50) Marakatti, V. S.; Halgeri, A. B. Metal ion-exchanged zeolites as highly active solid acid catalysts for the green synthesis of glycerol carbonate from glycerol. *RSC Adv.* **2015**, *5*, 14286–14293.

(51) Corma, A.; Fornes, V.; Forni, L.; Marquez, F.; Martınez-Triguero, J.; Moscotti, D. 2, 6-Di-Tert-Butyl-Pyridine as a probe molecule to measure external acidity of zeolites. *J. Catal.* **1998**, *179* (2), 451–458.

(52) Góra-Marek, K.; Tarach, K.; Choi, M. 2,6-Di-tert-butylpyridine sorption approach to quantify the external acidity in hierarchical zeolites. *J. Phys. Chem. C* **2014**, *118* (23),

12266–12274.

(53) Huang, M. M.; Kaliaguine, S. Zeolite Basicity characterized by Pyrrole Chemisorption: An Infrared Study. *J. Chem. Soc. Faraday Trans.* **1992**, *88* (5), 751–758.

(54) Yang, C.; Wang, J.; Xu, Q. Aluminated zeolites β and their properties II. Basicities of aluminated zeolites β: an FTIR study of chemisorbed pyrrole. *Microporous Mater.* **1997**, *11*, 261–268.

(55) Angelici, C.; Meirer, F.; van der Eerden, A. M. J.; Schaink, H. L.; Goryachev, A.; Hofmann, J. P.; Hensen, E. J. M.; Weckhuysen, B. M.; Bruijnincx, P. C. A. Ex Situ and Operando Studies on the Role of Copper in Cu-Promoted SiO2–MgO Catalysts for the Lebedev Ethanol-to-Butadiene Process. *ACS Catal.* **2015**, *5*, 6005–6015.

(56) Sushkevich, V. L.; Ivanova, I. I.; Taarning, E. Mechanistic study of ethanol dehydrogenation over silica-supported silver. *ChemCatChem* **2013**, *5* (8), 2367–2373.

(57) Shimizu, K. I.; Sugino, K.; Sawabe, K.; Satsuma, A. Oxidant-free dehydrogenation of alcohols heterogeneously catalyzed by cooperation of silver clusters and acid-base sites on alumina. *Chem. - A Eur. J.* **2009**, *15* (10), 2341–2351.

(58) Hayashi, Y.; Akiyama, S.; Miyaji, A.; Sekiguchi, Y.; Sakamoto, Y.; Shiga, A.; Koyama, T.; Motokura, K.; Baba, T. Experimental and computational studies of the roles of MgO and Zn in talc for the selective formation of 1,3-butadiene in the conversion of ethanol. *Phys. Chem. Chem. Phys.* **2016**, *18*, 25191–25209.

(59) Chung, M.-J.; Han, S.-H.; Park, K.-Y.; Ihm, S.-K. Differing characteristics of Cu and ZnO in dehydrogenation of ethanol: A deuterium exchange study. *J. Mol. Catal.* **1993**, *79*, 335–345.

(60) Cheong, J. L.; Shao, Y.; Tan, S. J. R.; Li, X.; Zhang, Y.; Lee, S. S. Highly Active and Selective Zr/MCF Catalyst for Production of 1,3-Butadiene from Ethanol in a Dual Fixed

Bed Reactor System. *ACS Sustain. Chem. Eng.* **2016**, *4* (9), 4887–4894.

(61) Ordomskiy, V. V.; Sushkevich, V. L.; Ivanova, I. I. One-Step Method for Butadiene Production. *Us 8921635 B2* **2014**, *2* (12), 5.

(62) Jones, M. D.; Keir, C. G.; Di Iulio, C.; Robertson, R. A. M.; Williams, C. V.; Apperley, D. C. Investigations into the conversion of ethanol into 1,3-butadiene. *Catal. Sci. Technol.* **2011**, *1* (2), 267–272.

Ethanol Conversion into 1,3-Butadiene by Lebedev Method over MTaSiBEA Zeolites (M= Ag, Cu, Zn)

Pavlo I. Kyriienko, Olga V. Larina, Sergiy O. Soloviev, Svitlana M. Orlyk, Christophe Calers, Stanislaw Dzwigaj

Synopsis

Doping of TaSiBEA with Ag, Cu or Zn allows increasing selectivity of the bioethanol-to-butadiene process through proceeding easier ethanol dehydrogenation.